Master's thesis

NTNU
Norwegian University of Science and Technology
Faculty of Engineering
Department of Ocean Operations and Civil Engineering

Emil Andrè Huseklepp Tunli

Virtual prototyping and analysis of an azimuth thruster using measurements and numerical simulation

Master's thesis in Master Naval Architecture
Supervisor: Henry Piehl
Co-supervisor: Marko Mikulec
June 2023

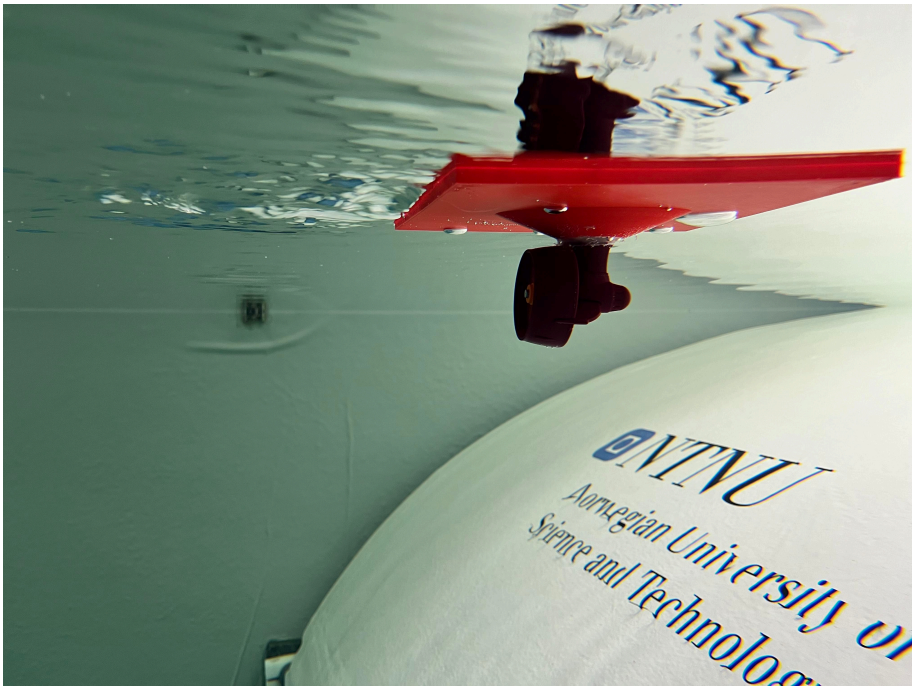

NTNU
Norwegian University of
Science and Technology

Emil Andrè Huseklepp Tunli

Virtual prototyping and analysis of an azimuth thruster using measurements and numerical simulation

Master's thesis in Master Naval Architecture
Supervisor: Henry Piehl
Co-supervisor: Marko Mikulec
June 2023

Norwegian University of Science and Technology
Faculty of Engineering
Department of Ocean Operations and Civil Engineering

NTNU
Norwegian University of
Science and Technology

Preface

This thesis concludes my five year education in naval architecture in the Norwegian University of Science and Technology (NTNU). This includes three year bachelor and two years master. The research was done in the towing tank of NTNU Ålesund.

The intended audience is engineers/designers interested in rapid prototyping, experiments and CFD. This thesis includes Creation of a real and virtual propeller geometry for testing in experiment and CFD.

I would like to thank my supervisor Henry Piehl and co-supervisor Marko Mikulec for all the assistance and help to develop my master thesis. I would also like to thank my student colleagues who helped me with my thesis work.

Thesis agreement

Background

There is an difference between real propeller geometry and the virtual propeller geometry. Computer assisted analysis of the propeller is therefore not necessarily that accurate for the real model. This difference can come from bad CAD drawings, manufacturing error, corrosion and erosion. This variance can have a large effect on propeller performance.

Motivation

Simulating real propeller geometry is useful in many cases. Propeller optimization is one of these. It is often difficult to know how great the distance is from cad geometry to real geometry.

Objective

The objective in this Thesis is to investigate and establish a procedure to create a virtual model of a real propeller. This includes reversed engineering and performance analysis for optimisation.

Research approach

The research is conducted with the following steps.

1) Parametric model
Create a model with the necessary parameters to fit the propeller. The model consist of main dimensions and sections with NACA profiles.

2) Rapid prototyping
A physical model with the same parameters as the virtual model will be created.

3) Experiment setup
A experiment setup consisting of a model thruster, motor, rotation sensor and force sensor will be made for testing.

5) Experiment An experiment in bollard pull condition will be run for a range of different rotation rates.

4) Virtual engineering
CFD will be done in similar conditions as the experiment.

5) Validation
A comparison between test results and CFD results will be done in order to verify the CFD result.

Abstract

This thesis investigates a methodology for establishing a virtual and physical experimental setup for testing a propeller in bollard pull condition. A virtual and a real physical geometry of a thruster was made. The real physical geometry was tested with an experiment for a range of different rotation rates. Force and rotation rate was measured. The virtual geometry is tested using computational fluid dynamics. Thrust force in direction of the propeller axis of rotation measured. The results was compared and it was found to be minor miss-match for 20-30rps while growing larger for higher rotation rates. It is not possible to distinguish the miss-match from the errors from computational fluid dynamics. Further research with a even more rigid CFD analysis will be needed.

Sammendrag

Denne master oppgaven undersøker en metodikk for å etablere et virtuelt og fysisk eksperimentelt oppsett for å teste en propell i bollard pull. En virtuell og en ekte fysisk geometri av en thruster ble laget. Den virkelige fysiske geometrien ble testet med et eksperiment for en rekke forskjellige rotasjonshastigheter. Kraft og rotasjonshastighet ble målt. Den virtuelle geometrien er testet ved hjelp av CFD. Skyvekraft i retning av propellens rotasjonsakse ble målt. Resultatene ble sammenlignet, og det ble funnet å være mindre mismatch for 20-30rps mens det ble større for høyere rotasjonshastigheter. Det er ikke mulig å skille miss-match fra geoemtri feil fra and feilkilder . Ytterligere forskning med en mer avansertanalyse vil være nødvendig.

Nomenclature

Term	Definition
Thrust	Force acting on an object in a certain direction.
Thruster	A device used to control motion and orientation of an object with thrust
rotation per second (RPS)	Number of rotation cycles made per second
Computational Fluid Dynamics (CFD)	Numerical method of calculating fluid flow using computational tool
Virtual modeling / computer assiset modeling (CAD)	Creation of a model using computational tool for modeling.
Rapid prototyping	Fast production of prototyping for testing and design.
Additive manufacturing	Creation of a product by adding material incrementally.
3D printing	Manufacturing by adding layer upon layer
Pulse Width Modulation (PWM)	Square pulse signal where the amount of each cycle is high voltage determines the value.
Analog signal	Signal where the value is determined by the property of the medium for communication
Incrementally	In regular steps.

Contents

1 Introduction

1.1 Background and motivation

A marine thruster utilizes a propeller to create thrust to maneuver a object in water. It creates a force in a similar way as a screw by rotating it pushes the water with a force and by the principle of Newtons third law of motion for every action there is an equal and opposite reaction. In fact the first propeller designs where based of screws such as the propeller on SS Archimedes which used an Archimedes screw.

Figure 1: Comparison between modern propeller and screws

Depending on the propeller rotation speed(rps) and ship velocity, a propeller is designed to provide a certain amount of thrust. An accurate prognosis of this thrust is one of the most crucial tasks for a Naval Architect. It directly influences the fuel consumption and maneuverability of the vessel. There is no analytical solution which works for every propeller. Numerical or experimental methods are therefore necessary. Experiments and CFD is some of the more advanced and convoluted methods possible and often comes with a large uncertainty. Statistical methods are needed in order to get a reliable outputs.

Experiments are often considered superior to simulations since it offers real physics. One drawback of experiments however is the cost and with large objects it becomes almost impossible. Another drawback is that experiments are extremely sensitive to interference and some measurements are almost impossible to do without disturbing the flow. Here Computational Fluid Dynamics (CFD) offers an advantage by being a computational tool in which measurements can be done without disturbing the system.

CFD also has some possible sources of error. The accuracy relies heavily on using correct physic models. It is often also not so certain that the virtual propeller geometry itself is the same as the real propeller geometry. There can be several factors that contributes to this difference. This can include inaccuracies in CAD drawings, manufacturing error as well as corrosion and erosion that occurs over time.

This thesis will investigate how these discrepancies affect the amount of output thrust. To research this, A CFD simulation and experiment will be compared with each other.

1.2 Objective

The objective of this thesis is to study a engineering methodology that combines computational fluid dynamics with experiment using reversed engineering and rapid prototyping. The main objective will be achieved by completing the following milestones:

1. Establish a parametric CAD model of a propeller suitable for 3D rapid prototyping and numerical simulation
2. Develop an experiment for measuring thrust and rotation rate on a model propeller.
3. Develop a CFD simulation on the virtual model for similar conditions as the experiment.

1.3 Thesis structure

The first milestone is achieved in chapter 3.1 by creating a virtual setup and a physical setup in order to do both experimental and virtual testing. The setup consist of a physical model Thruster and a virtual model using reverse engineering and rapid prototyping. The propeller is a virtual model which will be made into a physical by using rapid prototyping

Reversed engineering is used to create an accurate virtual model close as possible to the physical model. Since a propeller has a complex shape a virtual model of a different propeller is modelled and manufactured using 3D printing for use in the experiment. It is with this method easier to get a virtual model and a physical model which resemble each other.

The manufacturing of the physical propeller falls under the scope of rapid prototyping. This is also a technique which can be used further to manufacture and test different type of propeller. Additive manufacturing/3D printing is used in order to manufacture the propeller.

The second milestone is achieved in chapter 4.2 by doing experiment on the real propeller. The propeller is tested in an experiment where force and rotation is measured for different propeller rotations. The result will be used to create a empirical formula for thrust prediction.

The third milestone is achieved in 4.3 virtual engineering was done using Computational fluid dynamics. The limits of computational dynamics is the mesh, computational models and geometric shape. The CFD analysis results is used together with the experimental results as validation to get a deep understanding of the flow field and the propeller performance. This can then be used to find possible design improvements.

2 Theory

2.1 Modeling

The model consist of two parts the propeller and the thruster. The propeller will be made after the virtual model using additive manufacturing. The thruster house and nozzle is pre-made from another manufacturer.

Rapid prototyping is a method which allows a direct path from CAD to a real physical prototype[6]. This has real potential for testing of different design since making new prototypes is rapid and the cost is low. This is a concept used in this thesis.

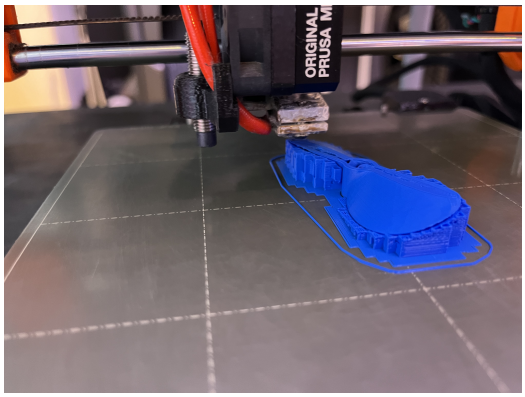

Figure 2: 3D printing thermoplastic PLA

Additive manufacturing is a way of manufacturing where a product is created by a process consisting of adding material incrementally often in layers. Additive manufacturing is often used together with rapid prototyping since the time from CAD to physical prototype is low. Additive manufacturing also allows manufacturing of complex geometries that would otherwise be very hard to manufacture. Possible drawbacks are the quality and accuracy of the prototype.

2.2 Experiment theory

Experiments require fine tuned instruments and control of the environment and external disturbances. International Towing Tank Conference [ITTC] guidelines [2] for open water testing was. It provides guidelines for how an experiment can be done of a thruster with nozzle and propeller. IT also describes how calibration should be done and how force should be measured.

The test and analysis is done in bullard pull condition ITTC Recommended Procedures and Guidelines Propulsion/Bollard Pull Test[3] goes through how such conditions should be measured and what possible physical conditions can be expected.

Measurements are combined by force measurements and rotation measurements. The force measurements are done with an analog strain gauge. The strain gauge uses a full bridge. This implements four elements that changes resistance when put under load.

The control signal for the propeller is pulse width modulation(PWM). PWM is a signal type which uses a square pulse duty cycle to communicate. The duty cycle is used to transfer a value. The value depends on how much of each time cycle is high voltage compared to low voltage.

2.3 Propeller theory

A marine propeller utilizes a rotating motion with foil shaped blades to create thrust to propel a vessel. The blades create lift and drag in a similar way as an airplane. The shape and angle of attack creates a pressure difference. The sum of the pressure will then act as a a thrusting force on the propeller, nozzle and hull.

The Thrust(T), Torque(Q), Rotation rate(n) and Propeller diameter(D) is used to calculate thrust coefficient(K_T) and torque coefficient(K_Q)

$$k_T = \frac{T}{\rho\, n^2\, D^4} \tag{1}$$

$$K_Q = \frac{Q}{\rho\, n^2\, D^5} \tag{2}$$

A marine propeller follows the same principle of pitch as a wood screw. For every rotation the screw advances one pitch distance[1]. This is not true for a propeller since it experiences slip since water is a fluid instead of a solid. A marine propeller usually has a more complex shape than a wood screw because water is slippery. This includes a few more parameters such as number of blades, blade area, rake, section shape, aerodynamic center of a propeller section, foil camber, cord length, rake and skew.

2.3.1 Geometry Design:

Defining the propeller blade shape is the first step. The area and volume distribution of the blade is defined by the sections. The chord length defines the length of each section.

The maximum thickness of each section is defined as a percentage of the chord length in the first two digit in the NACA-4 digit foil.

Pitch angle is derived from the pitch distance. The goal is to get a constant angle of attack in order to avoid creating pressure difference across the blade length.

$$\phi = \arctan\left(\frac{P}{2\pi r}\right) \tag{3}$$

2.3.2 Blade profile

A hydrofoil shape was used since it provides a proven way of creating lift and therefore thrust force. How a hydrofoil creates lift by motion through a fluid can be explained in two ways with use of Bernoulli's principle and Newtons law of motion.

Bernoulli's's principle states that there is a coupling in velocity and pressure. This can be used to explain foil-lift since an hydrofoil creates a velocity difference from the fluid above from the fluid bellow and therefore a pressure difference. The net force is the total pressure acting on the surface of the foil. The net force will act upwards as lift since the pressure on top of the wing is lower than the pressure bellow the wing.

Hydrofoil-lift can be explained by Newton's law of motion since the foil changes the direction of the momentum of the fluid. By Newtons second law a change in momentum requires a net force. By Newtons third law this net force creates an equal and opposite reaction force which acts as lift on the foil.

The sections of the propeller will consist of NACA 4 digit airfoils. The shape of the airfoil is defined by 4 digits[5]. The 4 digits are used in The first digit (M) defines the camber as a percentage of the cord. The second digit (P) defines the distance from maximum camber to the leading edge in tenths of the cord. The last tow digits (T) describes the maximum thickens as a percentage of the chord.

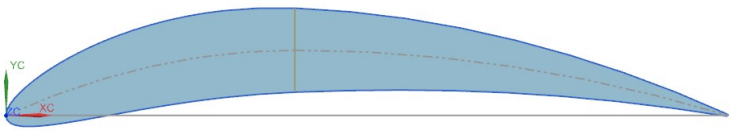

Figure 3: NACA 4 digit foil

a_0	0.2969
a_1	-0.126
a_2	-0.3516
a_3	0.2843
a_4	-0.1015

Table 1: Constants with no trailing edge

Leading camber

$$X_{cl} = tl\,P \tag{4}$$

$$Y_{cl} = \frac{M}{P^2}\left(2\,P\,X_{cl} - X_{cl}^2\right) \tag{5}$$

Trailing camber

$$X_{ct} = tt\,(1-P) + P \tag{6}$$

$$Y_{ct} = \frac{M}{(1-P)^2}\left((1-2*P) + 2\,P\,X_{ct} - X_{ct}^2\right) \tag{7}$$

Thickens at a given point

$$Y = \left(\frac{T}{0.2}\right)\left(a0\,X_c^{0.5} + a1\,X_c + a2\,X_c^2 + a3\,X_c^3 + a4\,X_c^4\right) \tag{8}$$

$$\theta_l = arctan\left(\frac{dy_l}{dx_l}\right) = arctan(0) \tag{9}$$

$$\theta_t = arctan\left(\frac{dy_t}{dx_t}\right) = arctan\left(\left(\frac{2\,M}{(1-P)^2}\right)(P - X_{ct})\right) \tag{10}$$

The following equations describe the curves at different sections of the foil

Upper leading edge

$$X_{ul} = L\left(X_{cl} - Y_{tl}\,sin(\theta_l)\right) \tag{11}$$

$$Y_{ul} = L\left(Y_{cl} + Y_{tl}\,cos(\theta_l)\right) \tag{12}$$

lower leading edge

$$X_{ll} = L\left(X_{cl} + Y_{tl}\,sin(\theta_l)\right) \tag{13}$$

$$Y_{ll} = L\left(Y_{cl} - Y_{tl}\,cos(\theta_l)\right) \tag{14}$$

Upper trailing edge

$$X_{ut} = L\left(X_{ct} - Y_{tt}\,sin(\theta_t)\right) \tag{15}$$

$$Y_{ut} = L\left(Y_{ct} + Y_{tt}\,cos(\theta_t)\right) \tag{16}$$

lower trailing edge

$$X_{lt} = L\left(X_{ct} + Y_{tt}\,sin(\theta_t)\right) \tag{17}$$

$$Y_{lt} = L\left(Y_{ct} - Y_{tt}\,cos(\theta_t)\right) \tag{18}$$

The equations are used to create parametric foil sections. By changing a few parameters the foil shape changes. This method provide an precise way of modeling a propeller.

2.4 Computational fluid dynamics

The Computational Fluid Dynamics (CFD) in this thesis utilizes finite volume method. It divides volume into volumetric cells to solve the physic equation numerically inside the cell. CFD has the benefit with offering better insight into the flow than experiment. CFD requires a large amount of computational capacity in order to solve complex flow cases and is often time intensive. There is no known method to do this analytically for all cases without making to many assumptions. CFD is therefore often the best alternative besides experiments until a solution is found for Naiver Stokes equation.

Computational fluid dynamic is commonly used to calculate fluid motion and the resulting forces. Finite volume method was used in this case, to calculate the flow created by the propeller and find the resulting force.

2.4.1 Governing equation models

CFD utilizes several equations in order to calculate the flow properties.

Conservation model uses the conservation of momentum, energy and mass in order to calculate the flow. Naiver Stokes equation is commonly used for this and was used in this thesis.

Segregated flow was used since it requires less computational resources. There is also no reason to believe that coupled flow models necessary since speed is generally low.

An additional equation must be used to calculate the flow next to a wall.The purpose of the CFD done in this thesis is to calculate the sum of force acting on the walls of the thruster and propeller. a wall equation incorporate the effect a wall has on the flow. The wall model uses non slip condition and boundary layer in order to calculate the flow on and next to a wall.

Turbulence commonly occurs after some distance as a flow passes next to a wall with a velocity. Turbulence occurs frequently in a fast rotating propeller. Realizable K-epsilon two layer turbulent equation was used. Turbulence occurs when a laminar flow field collapses into itself and creates unpredictable behavior and small vertices. An extremely fine mesh would be needed to solve this behavior. An additional turbulence equation utilizing statistical methods is therefore used. k-epsilon and Reynolds-average naiver stoke equation or RANS-equation is a commonly used method and was used for this thesis.

The Reynolds number on a propeller can be calculated using formula 19 [4]. Where ν is kinematic viscosity $n_{0.7}$ is rotational speed at 70% radius, $c_{0.7}$ is section length at 70% radius, V_A is advancing velocity it is zero in the case of bollard pull.

$$Re_{0.7} = \frac{c_{0.7}\sqrt{V_A^2 + (0.7\,\pi\,n_{0.7}\,D)^2}}{\nu} \tag{19}$$

The propeller is spinning rapidly and the flow is likely to fluctuate with time, a transient temporal model was therefore used.

The propeller is spinning while the domain is stationary. Two meshes was used one with rotation for the propeller and one stationary for the nozzle, thruster house and domain. Sliding interface was used for the interface between rotation motion of the propeller. The total mesh will consist of two parts one rotating part and one static part. The rotating part has a rotation motion and will simulate the propeller spinning.

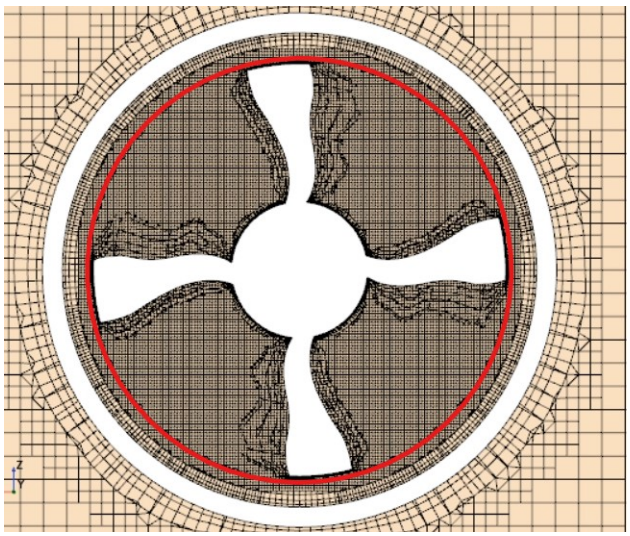

Figure 4: Picture of mesh with sliding interface marked in red. The picture is looking in towards the direction of the axis of rotation.

3 Methodology

3.1 Reversed engineering and rapid prototyping

The first step in the work for this thesis was to establish a physical and a virtual geometry for experiment and CFD. The setup up consist of a thruster base, a thruster house, a nozzle and a propeller.

Figure 5: Original setup

The modeling of the propeller consisted of trial and error with different modelling techniques. The first modelling technique used consisted of sketches modeled directly in the space of the blade. These defined the blade volumetric shape by creating an eclipsing surface defined by the sketches.

A technique using sketches on the center of the propeller projected on a cylindrical surfaces made the foil shape follow a circular path with the center in the propeller center. This is better for propeller performance since the foil shape appears with the apparent velocity. This was a tedious technique and allowed for easy human error.

The final modelling technique was with law curves following NACA 4-digit foil shape and with a value for the distance to the center and therefore also follow the apparent velocity. The law defined curves appears like the first technique in the space of the surface of the propeller blade. This technique allowed for a precise shape determined by mathematical formula.

There is some limitations in the 3D printing of the propeller. The trailing edge had to be larger than 0.2mm since the 3D printer was not able to print down to this level of detail.


[H]

Figure 6: Original propeller on left and new propeller on Right

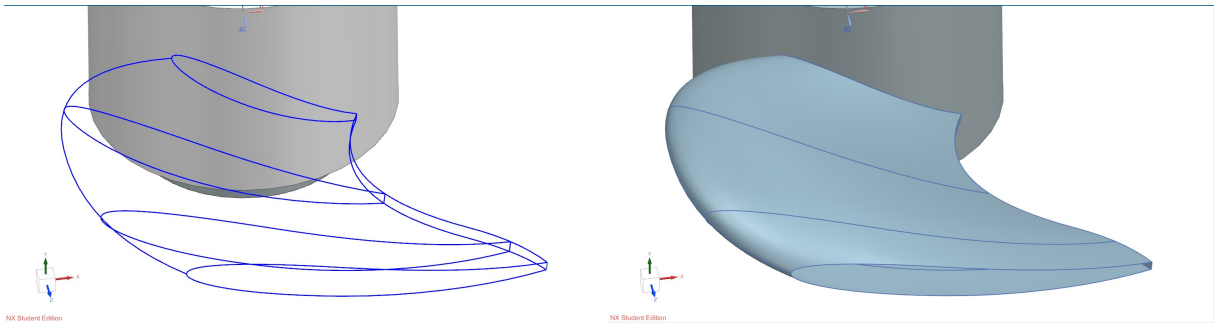

Figure 7: Creation of propeller blade from foil sections and spline guides

The virtual model is modeled after the physical experimental setup. The propeller diameter is 45mm and the pitch is 30 mm. It is not practical to include every minor detail since this would make the CAD file complicated and hard to incorporate into a volumetric mesh. The propeller is modelled using airfoil sections on the cross section of the blade. This sections is then used with sweep to create a body of the propeller blade.

3.1.1 Manufacturing

The propeller and the thruster mounting is manufactured using thermoplastic 3D printing a sub category of additive manufacturing. PLA(Polylactic acid) was used as infill/material.

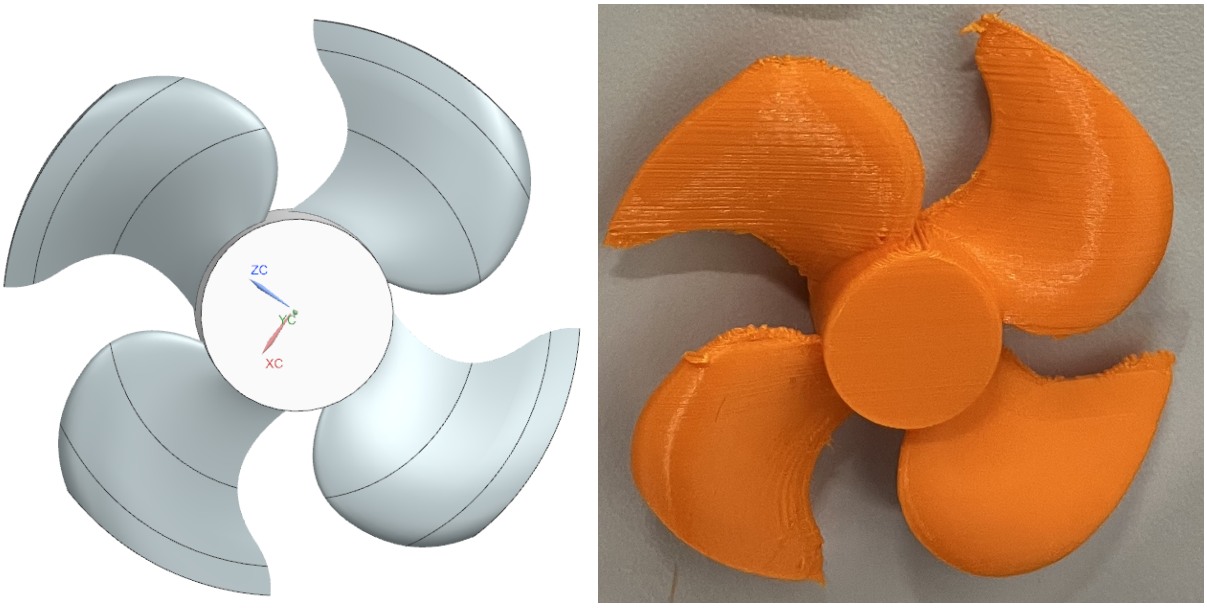

Figure 8: Physical and virtual model of propeller

The process from CAD geometry file to a real 3D printed object contains several steps. First a g-code has to be made. This code describes the motion of the 3D printing nozzle, temperature and extrusion speed. Several input variables determine the quality of the print such as layer height and thickness, object orientation, infill and support pattern.

The 3D printing had some final deviations from the virtual model. These are from the 3D printing. The 3D print accuracy, layer height and nozzle size limits the minimum tolerance possible. These imperfections are likely to cause a difference in thrust between the result from CFD and the experiment.

Figure 9: Picture of physical and virtual model

3.2 Test condition

The test conditions are made to be as close as possible for CFD and experiment. All conditions such as boundary condition, geometry and position was made to mach to a high degree. Even minor differences can have a large impact on the results it is therefore imperative to match the conditions as close as possible

The test is done in bollard pull condition. Bollard pull is when a propeller is spinning without advancing forward in the water. The flow field around the water will form a circular shape from the exit to the entrance of the thruster. This is because the water level and pressure equalizes. Since the thruster is pushing the water backward, the water around it has to move forward.

The total output force is measured on the complete sett-up in the water. This deviates from a standard open water bollard pull test where the propeller thrust is measured separately from the nozzle and thruster house. The thrust force value will be compared between CFD and experiment.

The rotation rate is the motion input for the CFD model and is constant. The rotation rate for the experiment is measured. The rotation rate was fluctuating in the experiment. This was countered by measuring the average force and average rotation rate with a large sample size. The average value was used together for different rotation rates to create a polynomial function as results.

The boundary condition consist of the tank wall and water surface. The water surface was assumed to be a wall for the CFD analysis. The water surface effect only seems to have an effect at higher rotation-rates where small ripples are starting to form. The tank is 8meters long, 2meters wide and 85 cm deep this is approximately 178 times longer, 44 times wider and 18 times deeper than the radius of the thruster. The distance from the outer boundary is large enough for assuming that the flow will not be disturbed by the outer boundary.

3.3 Experimental setup

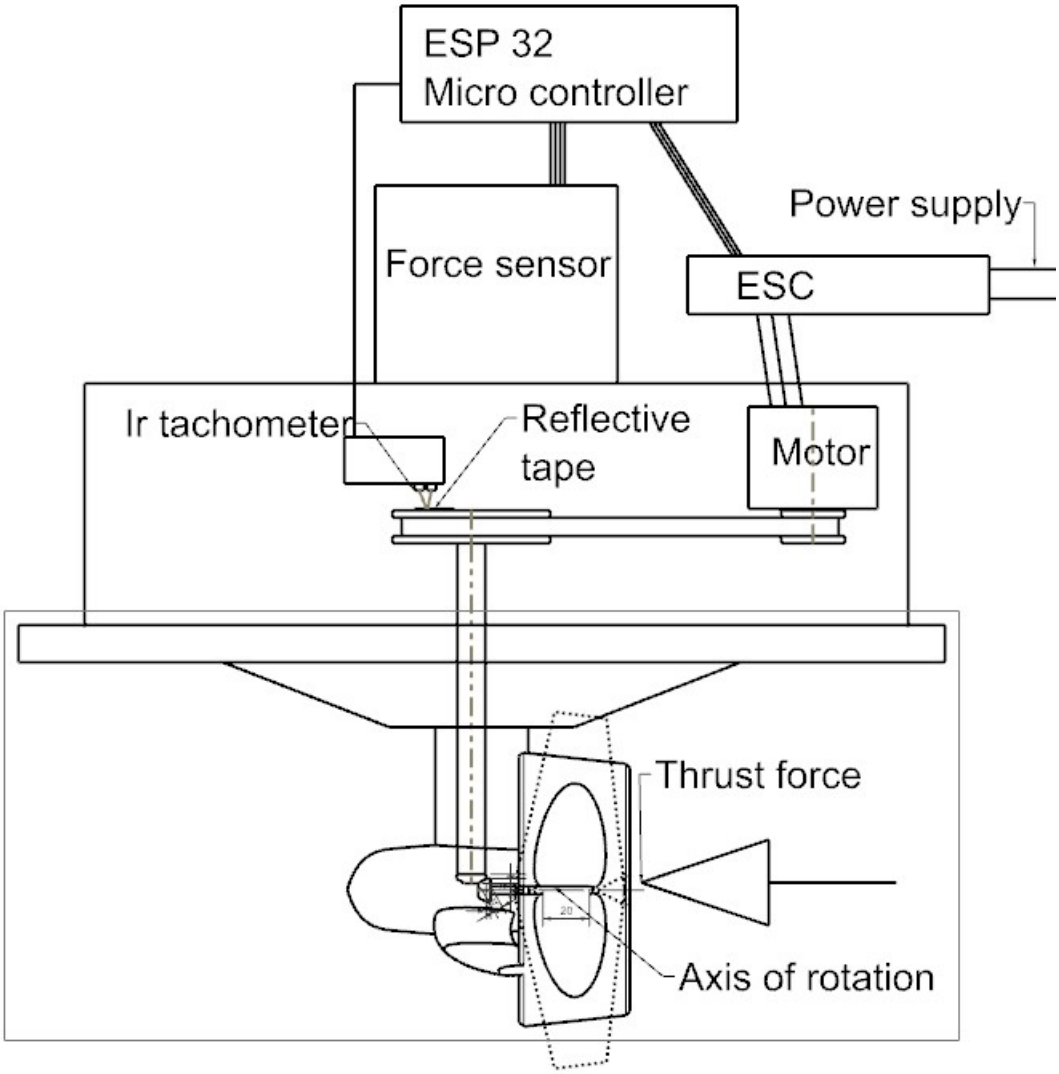

Figure 10: Sketch of the experimental settup

The objective of the experiment is to measure thrust force for a sett of different rpms. The results will be used to validate CFD analysis. The experimental setup consist of a 8x2x0.85m water tank a model thruster with nozzle, propeller, brushless DC motor with speed controller and a ESP32 micro-controller.

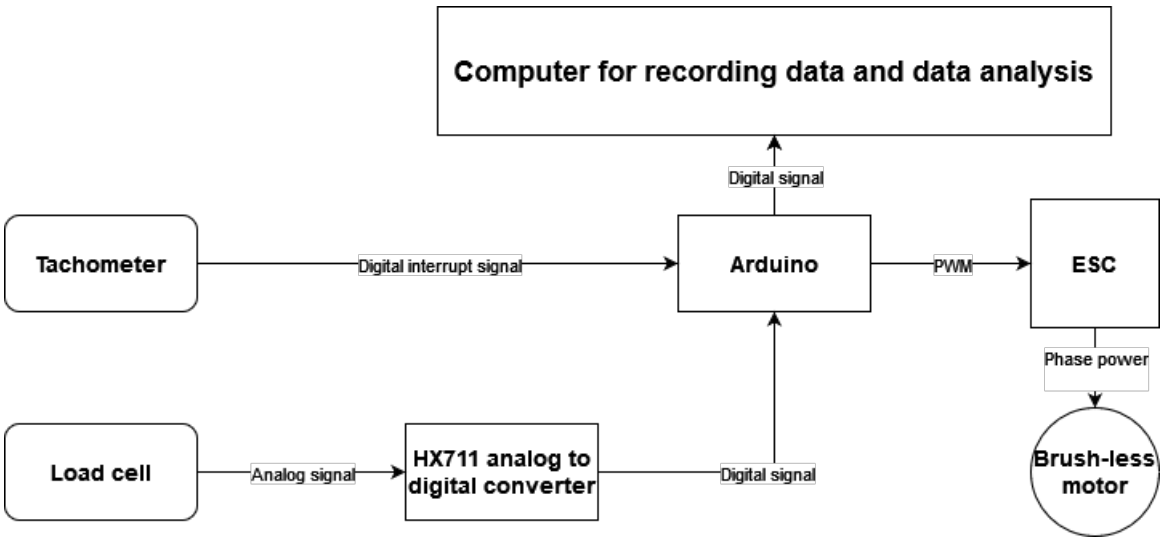

Figure 11: Signal and component diagram. An ESP-32 was used instead of an Arduino for the final experimental setup. Phase power is in the form of 3 alternating current power supply.

The sensors consist of a load cell sensor and a infrared tachometer. The micro controller receives values from the sensors combines them and send it to a computer for data processing.

A tachometer is used to measure the rotation rate. The tachometer senses reflective capacity of a element. It sends a infrared laser on a surface which reflects and is received by a infrared photo resistor. The potentiometer is tuned by a potentiometer to the right reflective sensitivity. The tachometer turns off when there is low reflection and on when there is high reflection. There is a black part and a yellow part on the axle. An interrupt routine is triggered in the Arduino when there is rising voltage. The Arduino calculates rotation rate by counting the number of interrupts per seconds and multiplying with the reduction rate of the gears.

The force measurement will consist of an analog load cell HBMS2M/1000 which will be measured by a HX711 analog to digital converter. The measurements output is sent to an esp 32 for processing and send the data to a computer for recording.

The load cell measure force with a set of 4 strain-resistors. The resistance varies as the wires expand and contract with strain. The force sensor consist of six output/input wires which can be connected to a analog measurement tool. A full bridge sett up was used since it provides a accurate and reliable analog reading. This sett-up consist of two positive and two negative voltage supply wires and two which are used to measure the force.

The rotation is measured in the experiment and used to find the relation between rotation rate and thrust force. The rotation rate fluctuates in the experiment in some rotation rates more than other. This is from imperfections in the gears causing periodical fluctuating forces. The amplitude grows larger for rotation rates matching the natural frequency of the system. A large amount of measurements will be taken for each PWM input and be used to calculate the average force and average rotation rate.

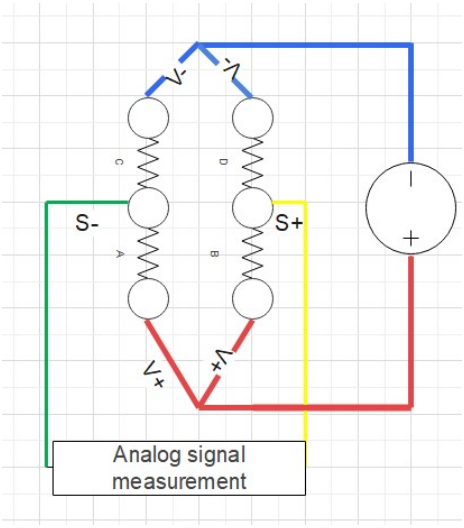

Figure 12: Circuit diagram of a Wheatstone bridge used for the load cell

A full bridge connection measures the analog electrical potential difference (volt) between the two signal wires as shown in figure 12. The analog output from the load cell varies as the Resistance in A, B, C and D varies by calibrating this signal can be made into a force measurement. The analog signal measurement are done with a HX7011 analog to digital converter. This converts the analog potential difference value into a digital value. This digital value is then sent to the Arduino for recording and data processing.

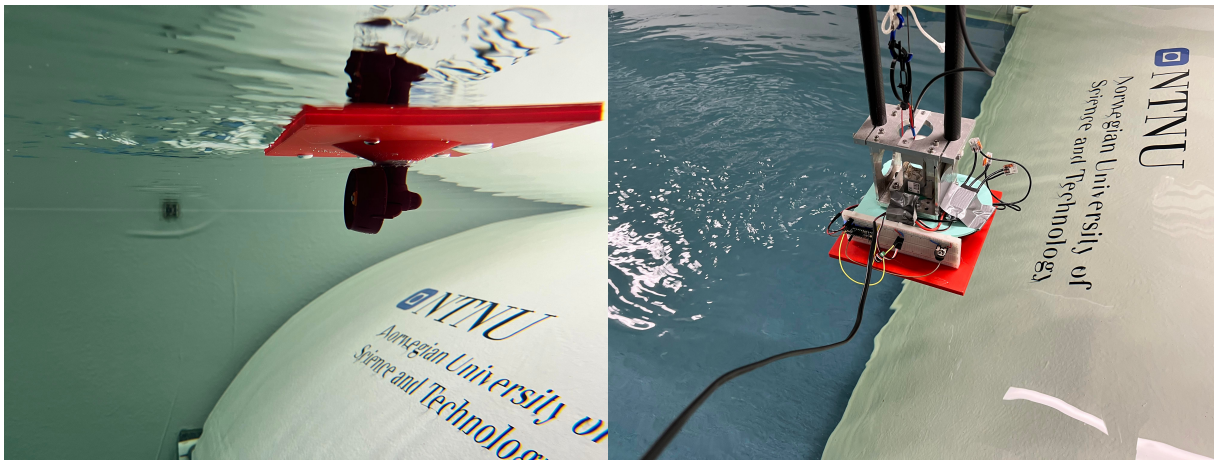

Figure 13: Setup in water

The micro-controller sends a pulse width modulation(PWM) signal to the ESC to power the motor which via a belt drives the propeller in a rotational motion. PWM sends an on off pulse the duty cycle is the percentage of time which the on cycle is to the total time. The library used in this case uses a value of 180 for 100% duty cycle and 0 for 0% duty cycle.

3.3.1 Calibration

Calibration is an integral part of the experiment. It is what connects the sensor readings to a metric unit of measurement. The force calibration procedure comprised two main steps: zero value determination and measurement of force increments. Static force was employed throughout the calibration process to ensure accurate and reliable results[2].

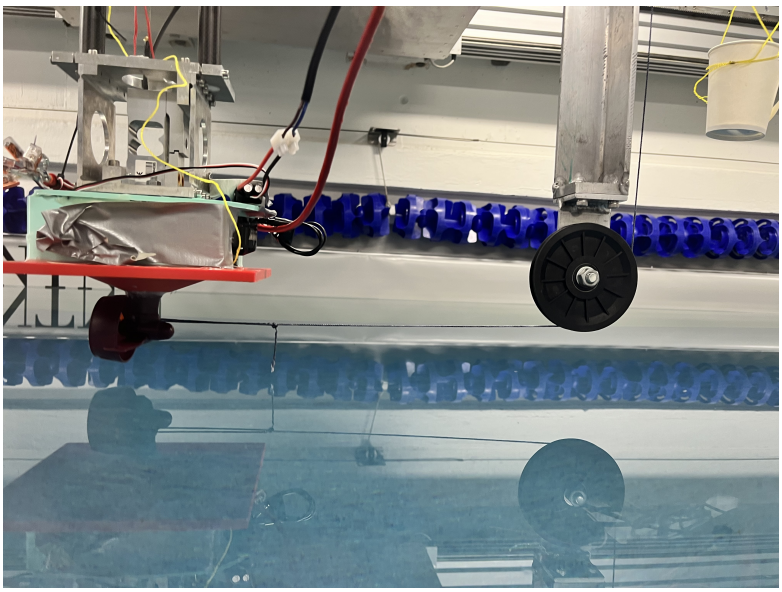

Figure 14: Picture of the calibration sett up. A line going from the thruster hub of the thruster to two pulley wheels with a cup where weights for finding the calibration gain value

To initiate the calibration, a zero mass is added to keep the rope tight and to get a consistent zero value to be used as offset. Subsequently, a series of 0.1 kg weights was added. The weight is applied in 6 steps, while the corresponding measurements are carefully recorded. This step-by-step approach allowed for the calculation of the gain and facilitated the analysis of trends within the recorded data.

A different offset is used in the experiment since the zero measurement is different. The offset for the thruster is found by measuring the force and calculating the average while the propeller is stationary.

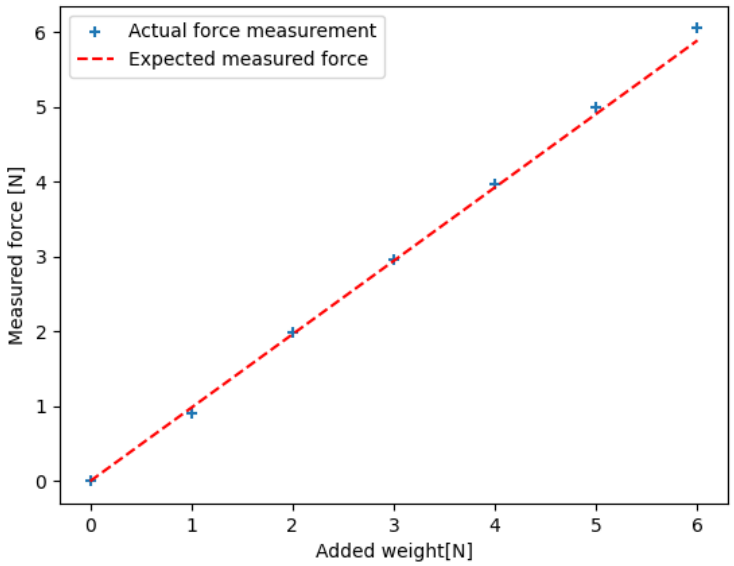

Figure 15: Calibration measurements calibrated with gain value. The relation between the measured force and added weight is linear and can therefore be calibrated with a constant gain.

$$T = D_{raw} \cdot G + C \tag{20}$$

Gain(G)	6.953E-06
Offset(C)	-433851.322

Calculation of force from raw data where D_{raw} is raw data, G is the gain value and C is the offset constant

The purpose of the force calibration process is to connect the measured raw data to a metric unit of measurement. By systematically increasing the force and observing the corresponding measurements, it was possible to assess the linearity, sensitivity, and overall performance of the system. The gained insights provided crucial information for the subsequent force measurements and ensured the validity of the experimental results.

3.3.2 Experimental test procedure

The experimental procedure comprises testing the propeller at various rotation rates to gather data for analysis. The thrust is a proportional function of the PWM signal. The test will be conducted by increasing the PWM signal incrementally to gather data for the hole range of rotations possible with the setup.

Prior to each test run, a calibration routine will be performed to verify and fine-tune the measurement setup. This calibration routine ensures the accuracy and reliability of the data acquired during the experiments, accounting for any instrumental variations or environmental factors.

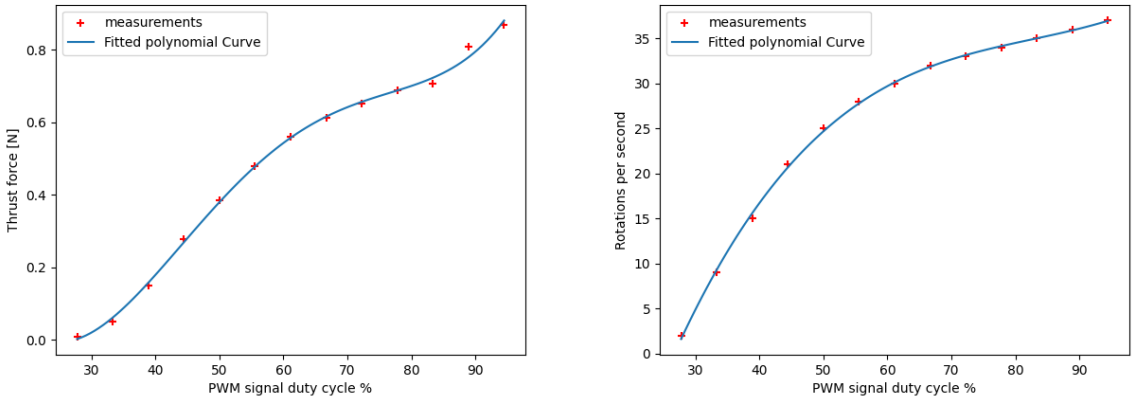

Figure 16: Average output from testing with incremental PWM duty cycle

The test was conducted in a series of steps with an incremental PWM signal. A PWM duty cycle of 28% was used as a start input. A 5% increase in duty cycle was used until 94% of duty cycle is reached. This was done in order to measure the relation between thrust and rotation.

By following this experimental protocol, which includes testing the propeller at different rotation rates. The propeller is tested for 200 seconds at each rotation rate. During each operation period 2700 measurements are done with a sample frequency of 13.5Hz. The amount of data samples insures an accurate average force calculation. The study aims to obtain precise and reliable data for analysis and investigation of the propeller's performance characteristics.

Time table

operation number	PWM duty cycle	average rotation rate	Operation period
1	28%	2 rps	200 seconds
2	33%	9 rps	200 seconds
3	38%	15 rps	200 seconds
4	44%	21 rps	200 seconds
5	50%	25 rps	200 seconds
6	56%	28 rps	200 seconds
7	61%	30 rps	200 seconds
8	66%	32 rps	200 seconds
9	72%	33 rps	200 seconds
10	77%	34 rps	200 seconds
11	83%	35 rps	200 seconds
12	88%	36 rps	200 seconds
12	94%	37 rps	200 seconds
TOTAL			40 minutes

Table 2: Operation time schedule

3.3.3 Measurement error

The measurement errors can come in the form of accuracy error or precision error. Accuracy errors can arise from factors such as incorrectly calibrated sensor setups and voltage fluctuations, leading to consistent deviations from the true values. To mitigate accuracy errors, a meticulous sensor calibration procedure will be conducted prior to the experiment. This procedure aims to align the sensor readings with the true values, minimizing any systematic inaccuracies that may impact the accuracy of the collected data.

Precision errors, on the other hand, involve random fluctuations in the measured values and can stem from various sources, including measurement system noise and sensor resolution limitations. While precision errors cannot be entirely eliminated, they can be quantified and minimized through statistical techniques and by conducting multiple measurements. To address precision errors, a robust approach will be adopted. Multiple measurements will be taken for each data point, increasing the sample size to capture the inherent variability and obtain a more comprehensive representation of the true value. Statistical analysis techniques, such as calculating the mean or average trend, will be employed to identify the central tendency of the measurements and reduce the impact of random fluctuations.

Throughout the experiment, great care will be taken to minimize both accuracy and precision errors. This will involve meticulous calibration procedures, including the calibration of sensors and measurement instruments, to ensure accurate and reliable readings. Additionally, measures will be implemented to stabilize the voltage supply, reducing the potential impact of voltage-induced errors on the measurements.

Special attention will also be given to minimizing sources of vibrations within the experimental setup. Isolation techniques, such as using vibration-damping materials and mounting the equipment on stable platforms, will be employed to reduce the influence of vibrations on the measurements. Furthermore, measures will be taken to shield the setup from external mechanical and electromagnetic disturbances that could introduce unwanted noise and affect measurement precision.

The collected measurements will undergo thorough documentation and analysis, including the quantification of accuracy and precision errors. This analysis will provide insights into the magnitude and impact of these errors on the experimental results. By carefully considering individual data points and overall trends, the study aims to ensure a reliable interpretation of the results and draw accurate conclusions regarding the propeller's performance.

By acknowledging and addressing accuracy and precision errors through meticulous calibration procedures, robust statistical analysis techniques, and measures to minimize external disturbances, this methodology ensures the accuracy, reliability, and validity of the experimental measurements.

3.4 CFD analysis

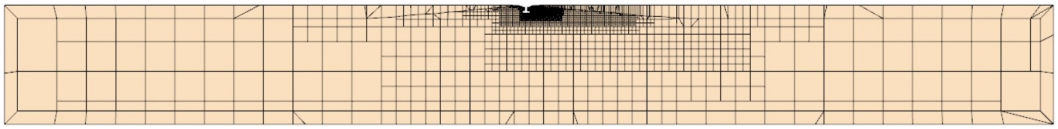

Figure 17: The total domain with refinement zones.

The objective of the CFD analysis is to obtain data that is impossible to measure in the experiment. This data consist of information of the flow field, torque on the propeller. This resulting data will be used to get a better understanding of the propeller and find possible design improvements.

The Reynolds number was used in the CFD simulation for finding a acceptable prism layer on the propeller.

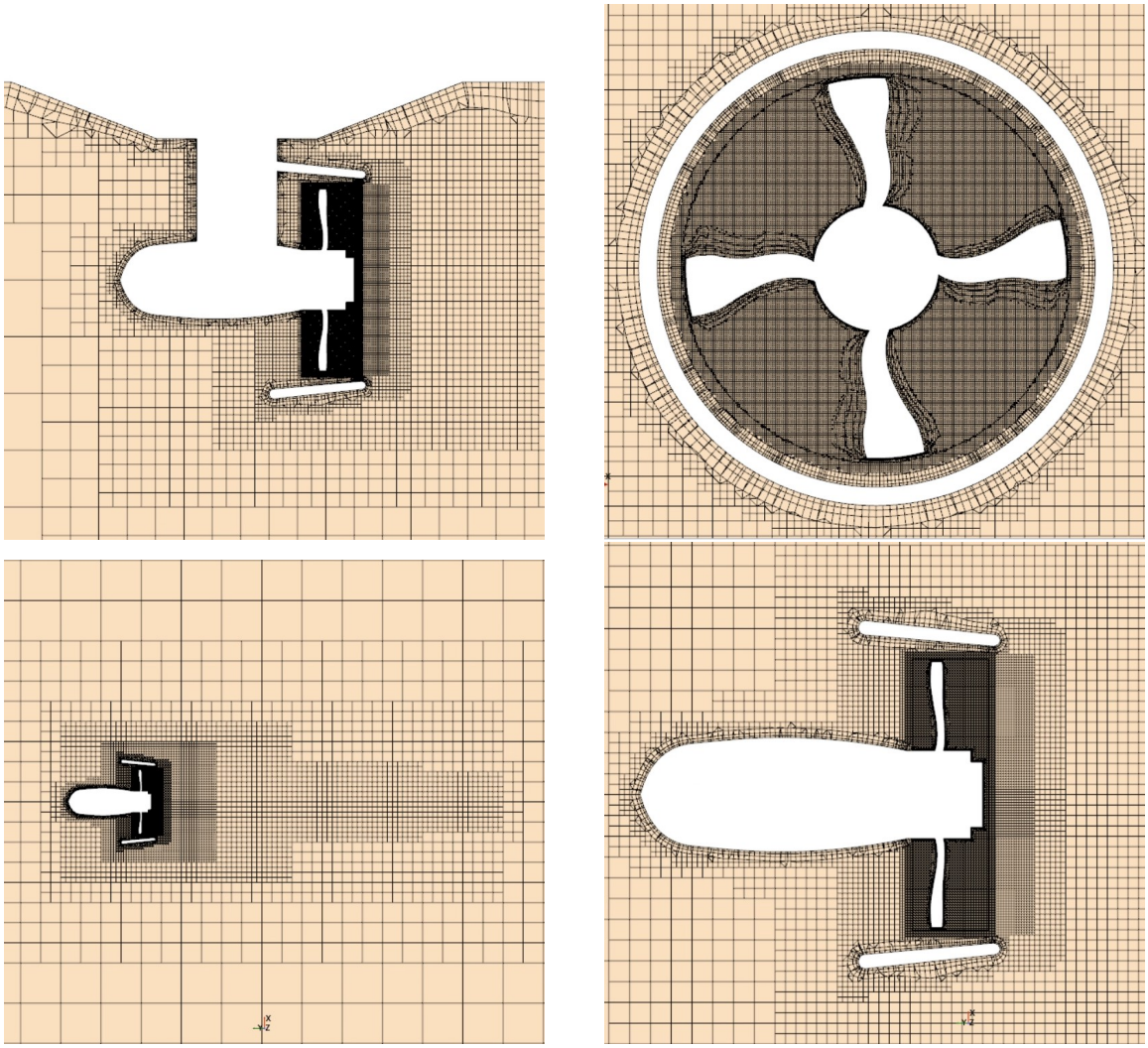

Figure 18: Mesh projection

A mesh convergence study was conducted but did not converge at a definite result. The mesh convergence study was neglected because of time restrictions. The CFD analysis will rather rely on validation with experimental result.

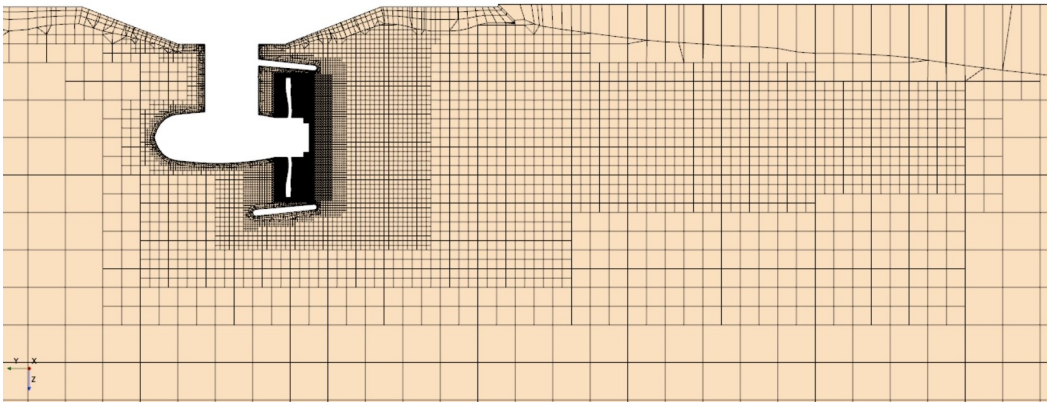

Figure 19: Mesh around the thruster and refinement zones

The geometry used in the CFD consist of the virtual geometry modeled after the thruster and the propeller geometry file used for 3D printing.The domain boundary is made to be of the same dimensions as the water-tank used in the experiment. The water surface was assumed to be a wall in order to save computational resources. The geometry is all together comparable with the environment used for the experiment.

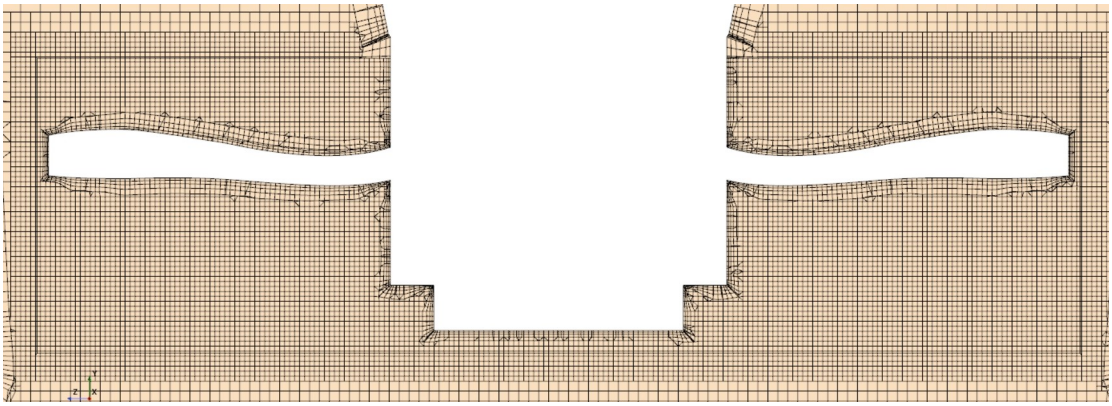

Figure 20: Mesh rotating domain

The CFD setup consist of two mesh domains. One domain consist of the rotating parts and the volume around it. This is the propeller domain this is where the most demanding meshing and analysis will be done. The other mesh is stationary and consist of the volume in the tank and around the thruster house.

	rotating mesh	stationary mesh	total
Number of cells	1.98E+06	1.31E+06	3.29E+06
Volume $[m^3]$	1.81E-05	1.44E+01	1.44E+01
representative cell length $[m]$	2.09E-04	2.22E-02	1.64E-02

Table 3: Mesh data

A CFD analysis for the same speeds and similar conditions as the physical experiments is done in order to get data that is impossible to obtain with experiment. A mesh study is done to find the optimal cell size and find its cell size sensitivity.

Time step size	0.0001 s
Inner iterations	5
Simulation time	5 s

Table 4: CFD analysis data

4 Results

4.1 Experiment

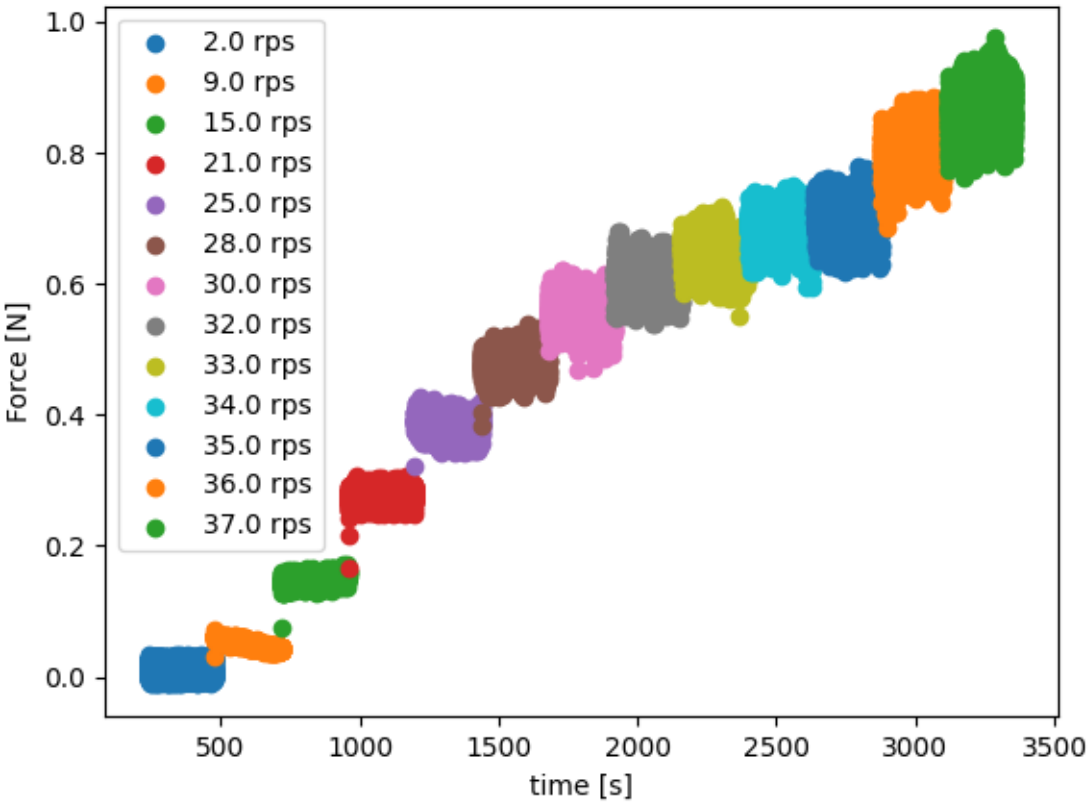

Figure 21: Caption

The force measurement in the experiment was done with a ESP 32. It has a capable processor able to receive and send signals at a fast rate. The readings are stable and has a little interference.

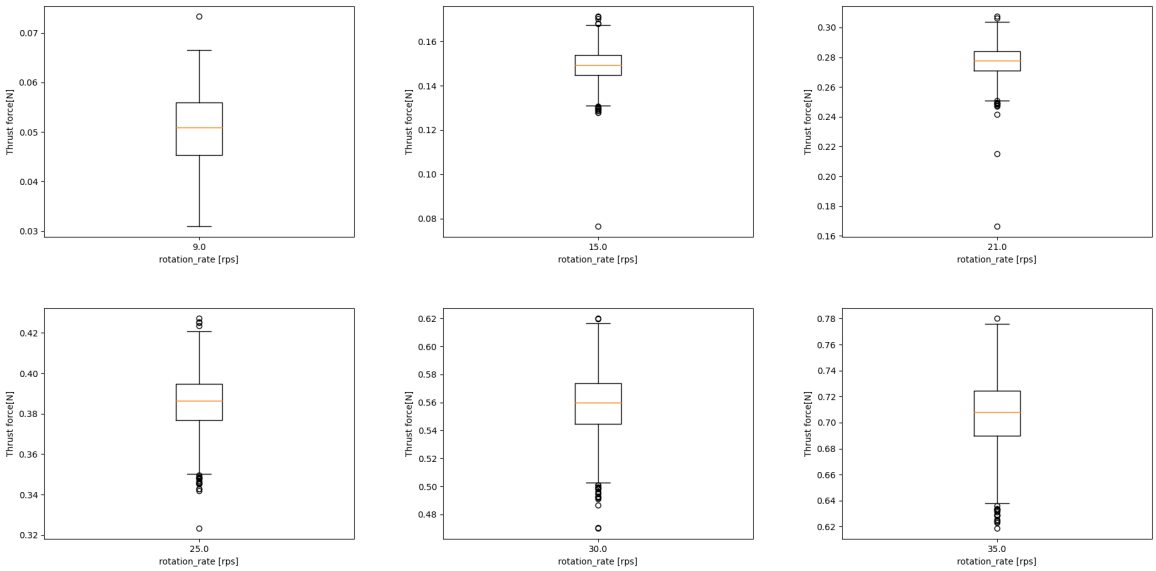

Figure 22: Box plot of force measurements for different rps. The plot visualizes the distribution of measurements values. The yellow line shows mean value, The box show the upper and lower quartile values of the data and outline 50% of the data, the whiskers mark the boundary for the range of data. The filler points marks the data outside the range.

The relation between thrust force T in newton and rotation rate R in RPS was found to be:

$$T = 0.0006035\,R^2 + 4.92 \cdot 10^{-5}\,R + 0.004428 \tag{21}$$

The relation between thrust force T in newton and PWM signal(P) was found to be:

$$T = 2.054e - 08\,P^4 + 8.912e - 06\,P^3 + 0.001344\,P^2 + 07458\,P + 1.358 \tag{22}$$

4.2 CFD result

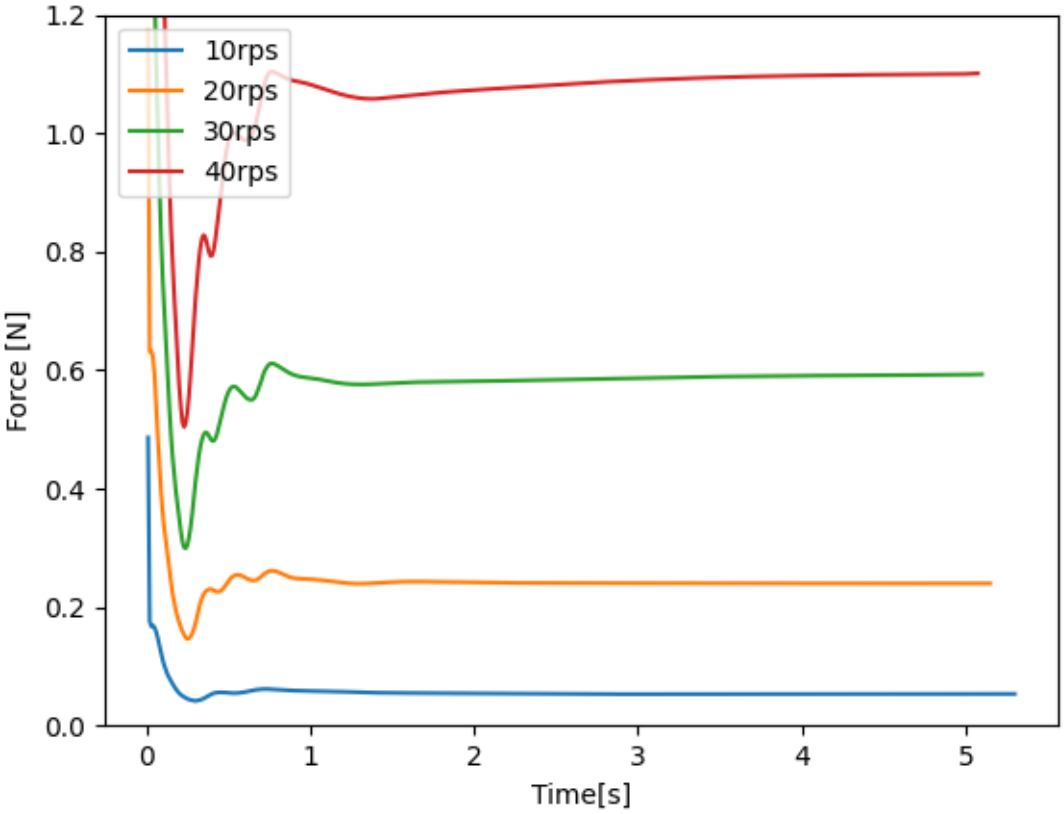

Figure 23: Thrust force time plot from CFD simulation.

The thrust force converged after 5 seconds simulation time. The thrust force used was the average of the last three rotations after 5second simulation time. This was to insure that any harmonic rotation effects in the force would offset the result.

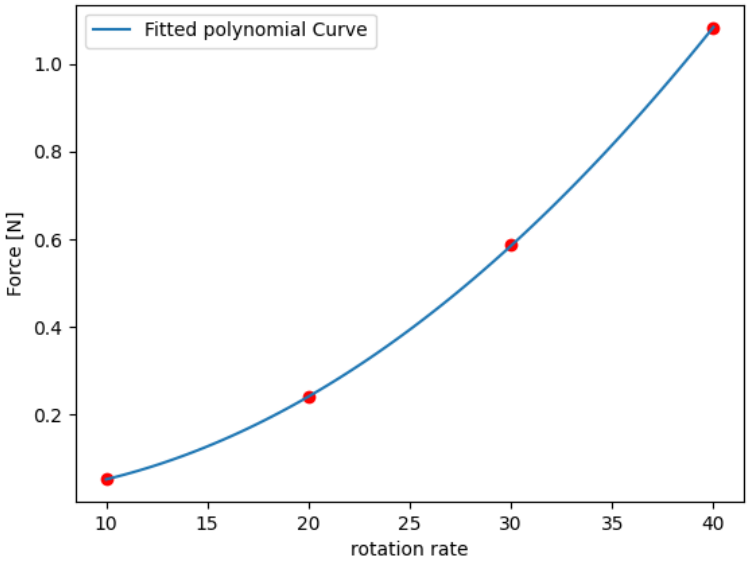

Figure 24: polynomial fitted curve to CFD results

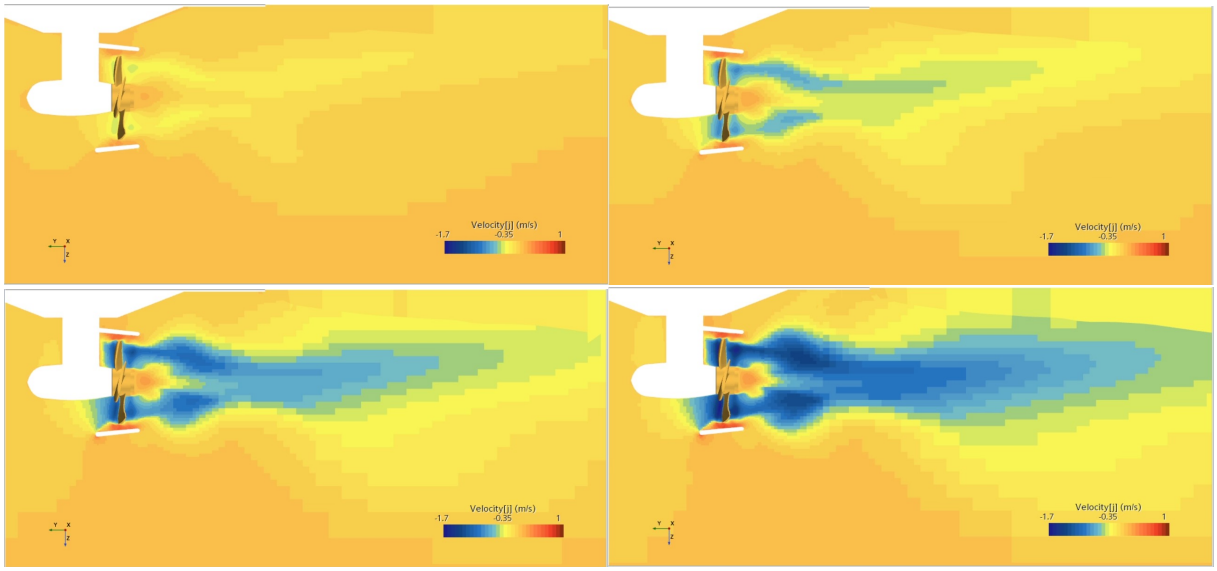

Figure 25: Velocity diagram from CFD. Top left is 10 rps, top right is 20 rps, bottom left is 30 rps and bottom right is 40 rps. The different diagrams use the same velocity color field. The diagram are at the end of the simulation after the force has converged. The flow field is not completely developed which is the reason for some unexpected flow patterns. The bulb is showing in the higher speed this is expected to go away if the simulation was given more time.

4.3 Comparison

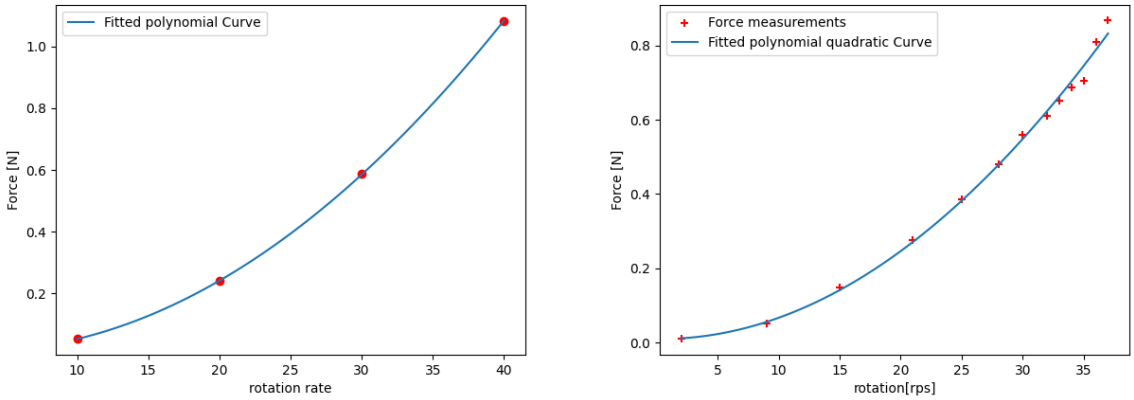

Figure 26: The one on the left shows the CFD results. Right shows experimental results. Data points are fitted to a polynomial function.

Rotation rate	Force CFD [N]	Force experiment [N]	Difference percentage
10 rps	0.05	0.07	20%
20 rps	0.24	0.25	3%
30 rps	0.59	0.55	7%.
40 rps	1.08	0.97	11%

Table 5: Comparison from CFD and experimetn

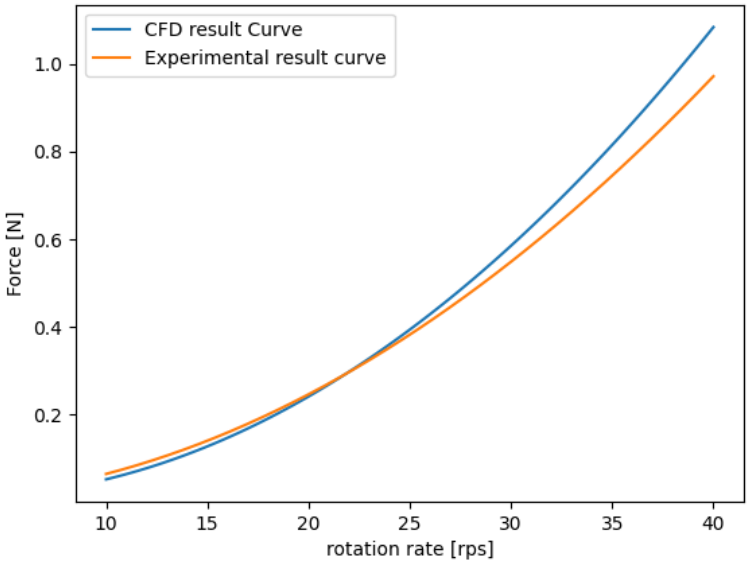

Figure 27: polynomial fitted curve to CFD results and experimental result

Rotation rate	Thrust coefficient CFD	Thrust coefficient experiment
10 rps	0.13	0.16
20 rps	0.15	0.15
30 rps	0.16	0.15
40 rps	0.17	0.15

Table 6: Thrust coefficient from experiment and CFD. The thrust coefficient is a non-dimensional value which can be used to calculate propeller thrust for a given diameter and rpm for a propeller with the same shape. The thrust coefficient should stay the same for different rotation rates.

$$k_T = \frac{T}{\rho\, n^2\, D^4} \tag{23}$$

$$K_Q = \frac{Q}{\rho\, n^2\, D^5} \tag{24}$$

5 Discussion

The results from CFD is comparable with the experimental result. For 30 rps the difference was 7% and down to 3% for 20 rps. For lower and higher rotations was the difference above 10% and up to 20%. This can be for a multitude of factors. For low rps it is likely that miss calibration has an effect. This might be more noticeable for lower rotation rates where a smaller calibration error would be larger compared the total measured value.

The 3D printing had some deviations from the virtual model. These occurred during the 3D printing. The details on the propeller is to small compared with the 3D printer accuracy, layer height and nozzle size. These imperfections are likely to cause a difference in thrust between the result from CFD and the experiment. It is however hard to distinguish the error from other sources of error.

The experiment has some potential sources of error. The rotation rate was fluctuating and this might have been from miss calibration The difference for smaller rotation rates are likely to be from There is a multitude of possible error that can arise from CFD. physic models, insufficient mesh refinement or wrongly defined boundary conditions are some possible sources of error in the virtual engineering.

The CFD analysis has some potential sources of error. The Y+ number is not the same for the different speeds. The y+ has a large effect on how the CFD model calculates the turbulent boundary layer properties. This is likely to cause some difference.

The water properties was not measured and it is therefore uncertain if they are the same for the CFD and the experiment. The water properties include viscosity and density which has a large effect on propeller performance. It is also possible water properties might be needed to include to get a matching CFD errors such as cavitation. Cavitation occurs when the pressure drops Bellow the pressure liquid/boiling point. It occurs more frequently at higher rotation rates. Cavitation was not included in this thesis because of limitations on time and resources.

The upper surface was assumed to be a wall instead of a free surface between water and air. This can have some effects especially on higher velocity when free water effects from the experiment was visible as waves.

6 conclusion

An engineering methodology using CFD and experiment was studied in this thesis. The methodology gave comparable results between CFD and experiment for mid range rotation rates (20-30 rps). For higher rps the difference grows larger. This is likely because of changing y+ value. The results from the comparison between the experiment and CFD were not able to estimate what the miss-matching geometry contributes with since other possible sources of errors clouds the results.A more controlled CFD analysis with a constant y+ value can make a clearer comparison possible. Further research will be needed.

The results and methodology can give ground for applications in the future. Work with iterative propeller prototyping and testing can be done using the methods described in this thesis.The CFD gave some additional information about the flow and can be assumed to be compatible with reality since validation with experiment. Improvements like decreasing the distance between the nozzle and propeller. The gap between propeller and nozzle large leading to circulation inside the nozzle which reduces efficiency. A possible improvement would be to increase the propeller diameter to match the nozzle diameter.

The results can be applied in DP application where a calculated amount of thrust can be given and therefore be able to counteract outside forces with outstanding efficiency and accuracy before the vessel is given time to move.

References

[1] JOHN CARLTON. “MARINE PROPELLERS AND PROPULSION SECOND EDITION”. In: (2006).

[2] ITTC. “ITTC – Recommended Procedures and Guidelines Open Water Test”. In: (2014).

[3] ITTC. “ITTC – Recommended Procedures and Guidelines Propulsion/Bollard Pull Test”. In: (2017).

[4] ITTC ITTC. “Recommended procedures Testing and Extrapolation Methods Propulsion, Performance Propulsion Test”. In: *Practical Guidelines for Ship Self-Pro- pulsion CFD* (2002).

[5] Jeff Scott. *NACA Airfoil Series*. URL: `https://aerospaceweb.org/question/airfoils/q0041.shtml`. (accessed: 02.06.2023).

[6] Xue Yan and PENG Gu. “A review of rapid prototyping technologies and systems”. In: *Computer-aided design* 28.4 (1996), pp. 307–318.

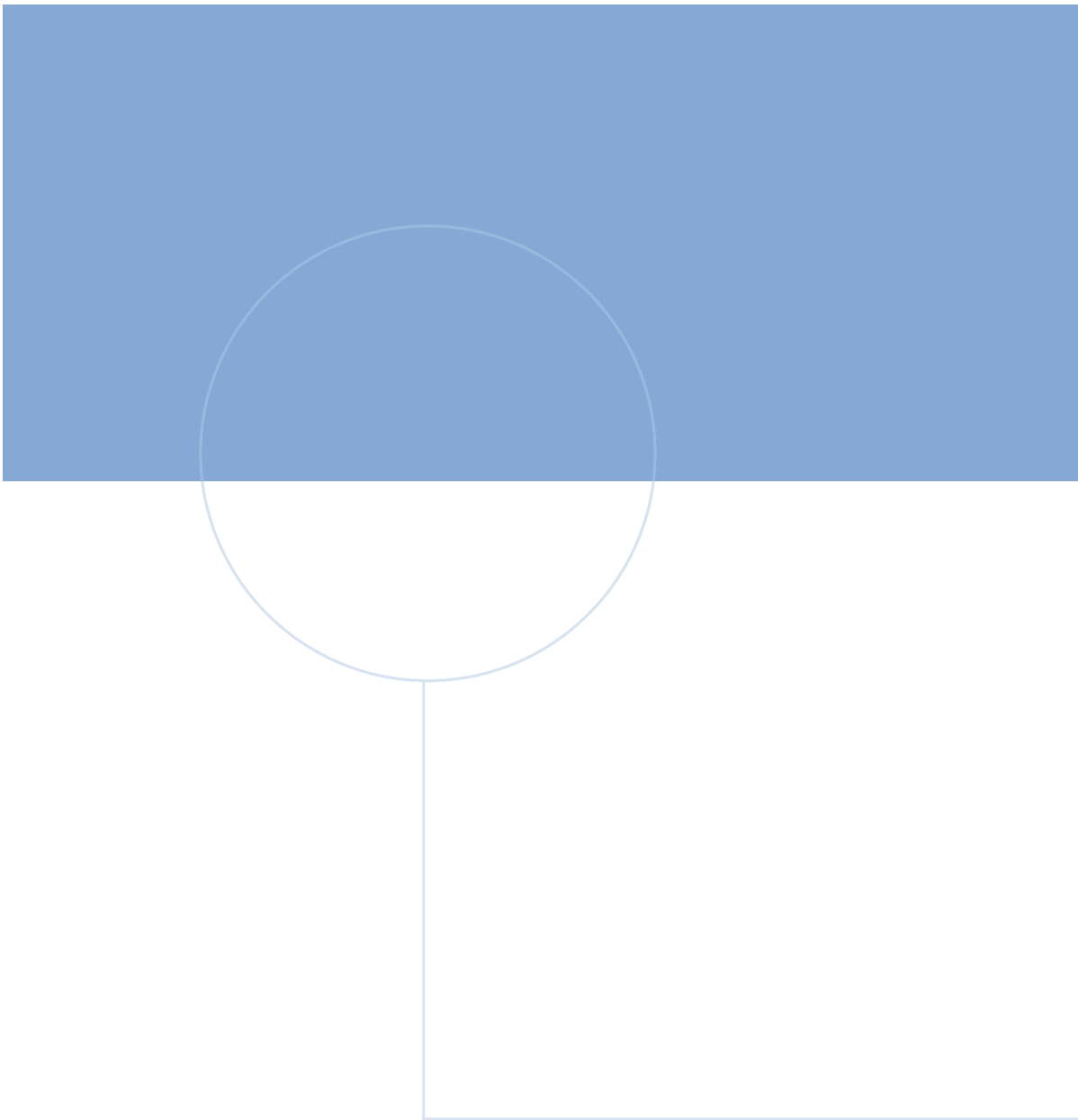

NTNU

Norwegian University of
Science and Technology